Anti-bacterial Test of $Sn_3O_4/TiO_2/SiO_2$ Particles with Controlled Sn_3O_4 Deposition

Akihiro Yamazumi, Dang-Trang Nguyen, Kozo Taguchi*

[1] Graduate School of Science and Engineering, Ritsumeikan University, Shiga, Japan.

* Corresponding author. Tel.: +81-77-561-5178; email: taguchi@se.ritsumei.ac.jp
Manuscript submitted December 15, 2021; accepted May 8, 2022.
doi: 10.17706/ijmse.2022.10.4.80-87.

Abstract: Photocatalysts are materials with high potential to solve the increasing environmental pollution problems and control viral growth. The most widely used photocatalyst, TiO_2, can utilize only 4% of sunlight as UV light, which has limited the scope of photocatalytic applications. Creating a photocatalyst that can be applied in the visible range will broaden the application of the material. We attempted to improve the photocatalytic performance by forming a heterostructure based on TiO_2/SiO_2 particles with improved light scattering properties and attached Sn_3O_4. The amount of Sn_3O_4 can be adjusted simply by controlling the hydrothermal synthesis time. As the hydrothermal synthesis time increases, Sn_3O_4 forms micro flowers on the TiO_2/SiO_2 surface. The photocatalytic performance was validated by bactericidal evaluation. It was confirmed that the presence of a small amount of Sn_3O_4 provided the highest bactericidal activity under fluorescent light irradiation.

Key words: Photocatalyst, visible light, anti-bacteria, bactericidal.

1. Introduction

Semiconductor photocatalysts are attracting significant attention as a potential solution to the growing global energy crisis and increasing environmental pollution problems due to their ability to sustainably convert solar energy into clean hydrogen fuel and to photochemically oxidize pollutants [1]-[3]. Titanium is the ninth most abundant material in the earth's crust, and is widely used in industry as a photocatalyst due to its low cost, high stability, and non-toxic characteristics. However, TiO_2 photocatalysts are activated only by high-energy ultraviolet (UV) light, which accounts for only 4% of sunlight, and thus do not perform well in indoor environments, greatly limiting their applicability [4]. Therefore, the search for high-performance photocatalytic materials that enable the use of visible light has been undertaken worldwide. WO_3, Ag_2O, PbO_2, etc. have been discovered as visible light-responsive photocatalytic materials, but due to their high cost and toxicity to the human body, they have not been widely used in industry [5]-[9].

Recently, the formation of Sn_3O_4 around TiO_2 has been reported to have visible light photocatalytic activity, and manipulation of the Sn_3O_4 shape has been reported to improve further visible light responsiveness and battery electrode performance [3], [10]-[14]. TiO_2 has also been structurally modified into one-dimensional nanorods, nanowires, nanobelts, nanotubes, and two-dimensional nanosheets and nanoplates have been formed to improve the performance of TiO_2 [15]-[19]. Among them, the core/shell structure of TiO_2 around SiO_2 particles and SiO_2-etched hollow spheres have been reported to improve light utilization efficiency and increase surface area, resulting in enhanced photocatalytic activity and electrode

performance [20]-[22].

In this study, we have prepared TiO_2 and Sn_3O_4 heterostructured particles for further visible light photocatalytic activity in indoor environments. By combining TiO_2/SiO_2 core-shell structure particles with Sn_3O_4 by hydrothermal synthesis, we confirmed that the presence of an appropriate amount of Sn_3O_4 contributes to the improvement of microbial disinfection performance under fluorescent light. Thus, we believe that photocatalysts that can utilize the ultraviolet and visible light contained in fluorescent lamps will have practical value in hydrogen production and decomposition of organic matter and bacteria.

2. Methods

2.1. Materials

Ethanol (C_2H_5OH, concentration 99.5%), Tetraethyl orthosilicate (TEOS, $(C_2H_5O)_4Si$), Ammonia (NH_3, concentration 25%) Acetonitrile (CH_3CN), Titanium tetraisopropoxide (TTIP, $[(CH_3)_2CHO]_4Ti$) Tin chloride dihydrate ($SnCl_2 \cdot 2H_2O$), Trisodium citrate dihydrate ($C_6H_5Na_3O_7 \cdot 2H_2O$), Sodium hydroxide (NaOH), 10% Nafion dispersion solution (DE1021 CS type), Butyl acetate, Sodium chloride were purchased from Wako Chemicals. Tryptone, Yeast extract were purchased from Becton, Dickinson and Company. All chemicals were used in their original form without purification. Deionized water was used in this study.

2.2. Synthesis of Photocatalysts

Sn_3O_4-deposited TiO_2/SiO_2 particles were prepared in two steps: (1) Preparation of TiO_2/SiO_2 core/shell structure nanoparticles: 48 ml of ethanol and 4 ml of deionized water were mixed and stirred at a water temperature of 40 ℃ for 30 min. Then 4 ml of ammonia water and 4 ml of TEOS were added to the mixture of ethanol and deionized water and stirred for 6 h to obtain SiO_2 colloidal solution. 24 ml of ethanol and 12ml of acetonitrile were added to the SiO_2 colloidal solution and stirred for 10 min. 6 ml of TTIP was slowly added dropwise using a syringe and stirred overnight. The products were separated by centrifugation 10000 rpm, 20 minutes, washed twice with deionized water and once with ethanol, and the obtained particles were dried at 60℃ for one day. After that, the obtained particles were calcinated at 450℃ for 7 hours; (2) Synthesis of $Sn_3O_4/TiO_2/SiO_2$ particles [12]: Add 1.14 g of $SnCl_2 \cdot 2H_2O$ and 3.68 g of $C_6H_5Na_3O_7 \cdot 2H_2O$ to 12.5 ml of deionized water and stir for 5 min to obtain a clear solution. 0.238 g of the particles produced in (1) and 12.5 ml of 0.2 M NaOH were added to the as-prepared solution and sonicated for 15 min. The solution was transferred to a 100 ml Teflon-lined stainless steel autoclave, and hydrothermal synthesis was carried out in four patterns at 180 ℃ for 5, 7, 12, and 15 hours. The resulting powder was washed multiple times with deionized water and dried at 60 ℃ for 24 hours.

2.3. Preparation of Photocatalytic Coated Glass

2 ml of Nafion and 3 ml of butyl acetate were mixed, and then 1.5 g of the prepared powders was added and stirred for 6 hours. Each mixture was coated on three 20 mm x 20 mm glass slides using a spin coater. The prepared glass slides with photocatalysts were dried at 60 ℃ for 24 hours.

2.4. Anti-bacterial Test

To prepare LB solution, 5 g of tryptone, 2.5 g of yeast extract, and 5 g of sodium chloride were added to 400 ml of deionized water and mixed. After that, 6 ml of 0.32 M NaOH solution was added to the solution, and deionized water was added to make 500 ml of the total solution. The as-prepared LB solution was sterilized by autoclaving and stored in a refrigerator for one day. 0.0015 g of dry yeast powder was added to 50 ml of the LB solution and incubated in an incubator at 35 ℃ for two days. 1 ml of the cultured bacterial solution was added to 9 ml of deionized water to prepare a 10-fold diluted bacterial solution. 30 μl of 10-fold diluted bacterial solution was dropped onto each glass slide coated with TiO_2/SiO_2 and

$Sn_3O_4/TiO_2/SiO_2$ photocatalyst with hydrothermal synthesis time of 5, 7, 12, and 15 hours, respectively, and a cover glass was placed on top. The glass slides with the bacterial solution were left under fluorescent light for 6 h. After that, the cover glass and glass slides were washed with deionized water, and 0.1 μl of the washing solution was dropped onto the agar medium and applied to the entire agar medium surface by a bacteria spreader and kept in an incubator set at 35 ℃ for two days. The photocatalytic performance of each photocatalytic sample was evaluated by observing the colonies formed on the agar medium. This test was conducted three times.

3. Results and Discussion

3.1. Structure of Photocatalyst

The morphology of TiO_2/SiO_2 particles and $Sn_3O_4/TiO_2/SiO_2$ particles was observed using SEM.

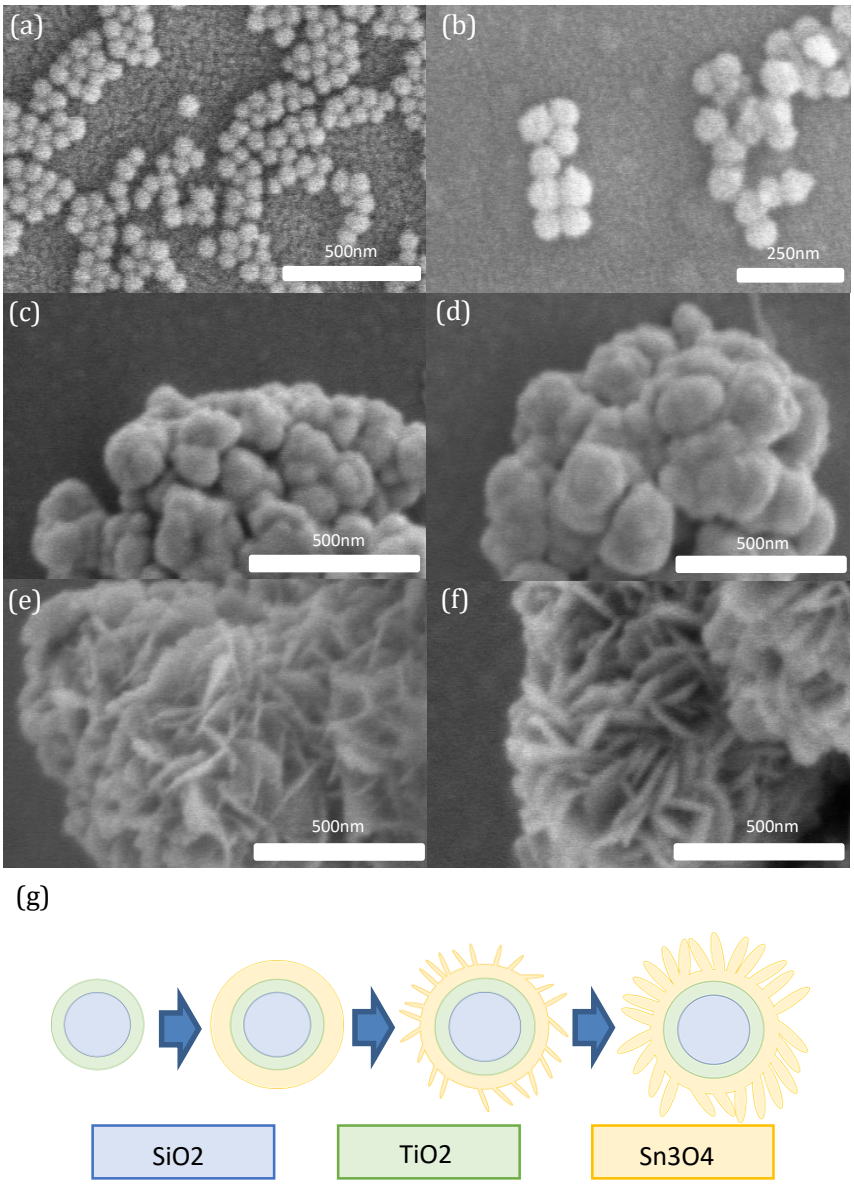

Fig. 1. SEM images of (a) SiO_2 particles, (b) TiO_2/SiO_2, (c) $Sn_3O_4/TiO_2/SiO_2$ hydrothermally reacted for 5 h, (d) 7 h, (e) 12 hours, (f) 15 hours, (g) image of the synthesis process of Sn_3O_4.

Fig. 1 shows SEM images of (a) SiO_2, (b) TiO_2/SiO_2, (c) $Sn_3O_4/TiO_2/SiO_2$ hydrothermally reacted for 5 h, (d)

$Sn_3O_4/TiO_2/SiO_2$ hydrothermally reacted for 7 h, (e) $Sn_3O_4/TiO_2/SiO_2$ hydrothermally reacted for 12 h, and (f) $Sn_3O_4/TiO_2/SiO_2$ hydrothermally reacted for 15 h. The particle size of SiO_2 is distributed in the range of 30 nm to 60 nm (Fig. 1 (a)), the particle size of TiO_2/SiO_2 is distributed in the range of 50 nm to 80 nm, and the thickness of TiO_2 film on SiO_2 particles is formed from a few nm to a dozen nm (Fig. 1 (b)). The SEM images after the hydrothermal reaction in Fig. 1 (c), (d), (e) and (f) are all agglomerated, which is thought to be due to the formation of Sn_3O_4 in the precipitated and deposited TiO_2/SiO_2 particles during the hydrothermal reaction. Fig. 1 (c) shows the initial stage of Sn_3O_4 formation, where the form gradually covered the surface of TiO_2/SiO_2 particles. In Fig. 1 (d), the Sn_3O_4 coating progressed further and increased thickness while aggregating with the surrounding particles. In Fig. 1 (e), the Sn_3O_4 seeds coated on the TiO_2/SiO_2 particle surface grew into a micro-flower structure distributed in the thickness range of several nm to 20 nm. In Fig. 1 (f), it can be observed that the Sn_3O_4 micro-flower grew in size and distributed in the range of 20 nm to 50 nm in thickness. Fig. 1 (g) shows an image of the synthesis process of Sn_3O_4 when using TiO_2/SiO_2 particles, showing that the morphology of Sn_3O_4 on the surface of TiO_2/SiO_2 particles can be easily controlled by preparing the hydrothermal synthesis time.

3.2. Anti-bacterial Test

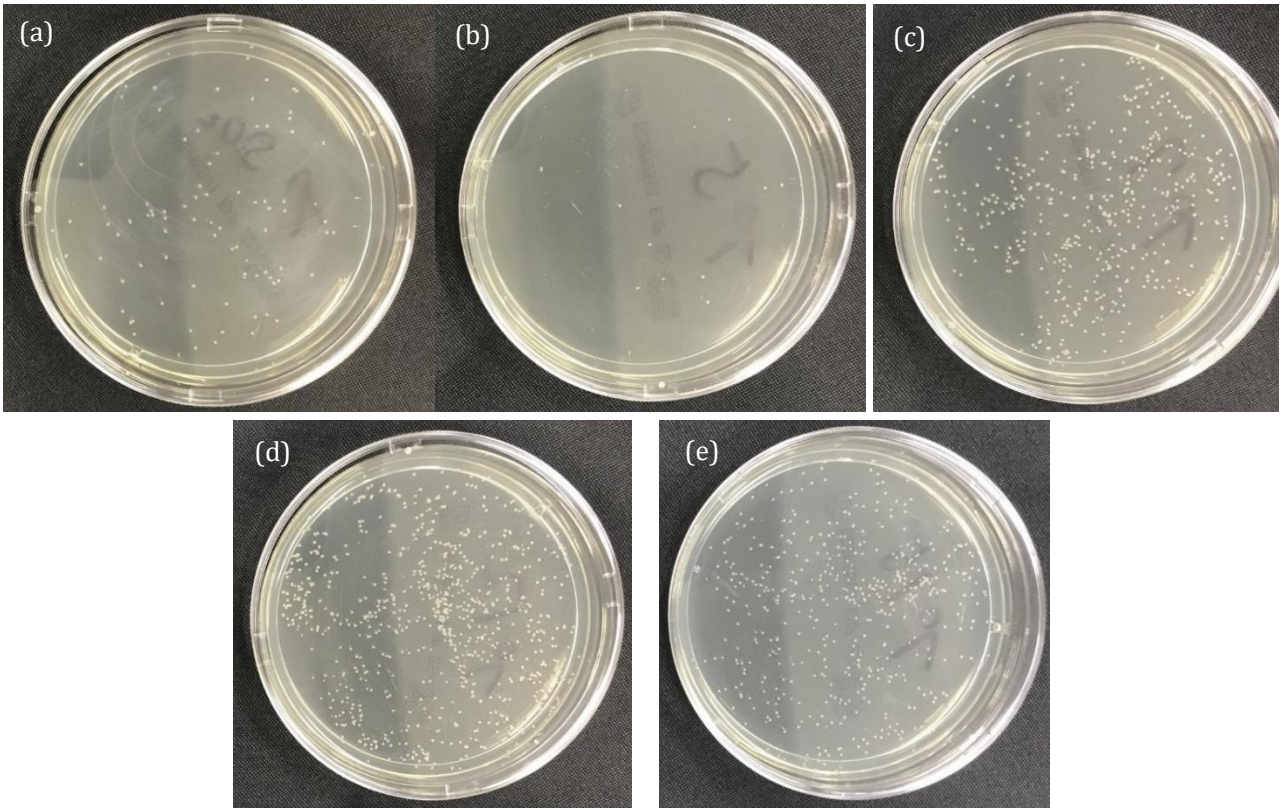

Fig. 2. Images of agar medium after 1 day of (a) TiO_2/SiO_2, (b) $Sn_3O_4/TiO_2/SiO_2$ hydrothermally reacted for 5 h, (c) 7 h, (d) 12 h, (e) 15 h.

Table 1. The Average Number of Colonies in Three Anti-bacterial Tests

Types of photocatalysts	Count of colony
TiO_2/SiO_2	124
5h $Sn_3O_4/TiO_2/SiO_2$	11

Fig. 2 shows images of agar mediums one day after they were applied with the bacterial solutions collected after the sterilization tests. Table 1 shows the number of colonies formed on the agar medium. It

was observed that the number of yeast colonies formed by the $Sn_3O_4/TiO_2/SiO_2$ particles hydrothermally synthesized for 5 hours showed the highest bactericidal performance with an average of 11 colonies.

The TiO_2/SiO_2 particles were next in line, followed by the particles hydrothermally synthesized for 7 hours and the difference in bactericidal performance between them. This difference in the bactericidal evaluation test can be attributed to the difference in the degree and morphology of Sn_3O_4 coverage.

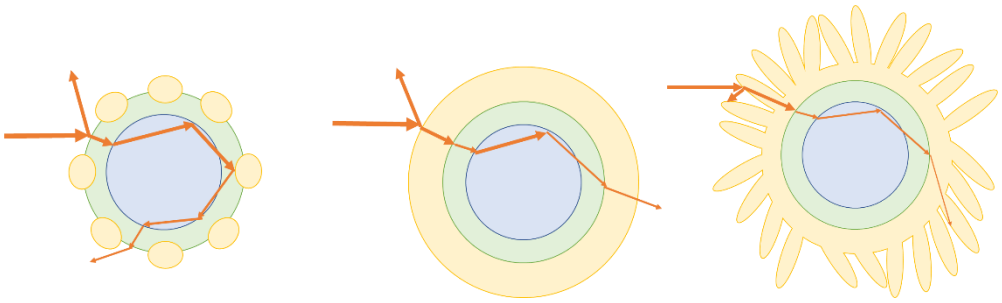

Fig. 3. Schematic of the path of light in a particle structure (Arrows indicate the path of light).

Fig. 3 shows a schematic diagram of light scattering [22]. The particles used in this study have a TiO_2/SiO_2 core-shell structure, which improves the efficiency of light energy utilization by confining light and increasing the length of the absorption path [20]-[22]. Therefore, in the case of particles with short hydrothermal reaction time, light is sufficiently irradiated to TiO_2 and Sn_3O_4, respectively, enabling them to improve their performance as photocatalysts. Sn_3O_4 has a bandgap of 2.61 eV in the visible region (2.3-2.8 eV), which makes it visible light-responsive, whereas TiO_2 has a bandgap of 3.26 eV, which makes it not visible light-responsive, and the lower conduction band (CB) and upper valence band (VB) potentials of Sn_3O_4 are both higher than the potentials of VB and CB of TiO_2. Therefore, the heterostructure of Sn_3O_4 and TiO_2 is a type II heterojunction [23].

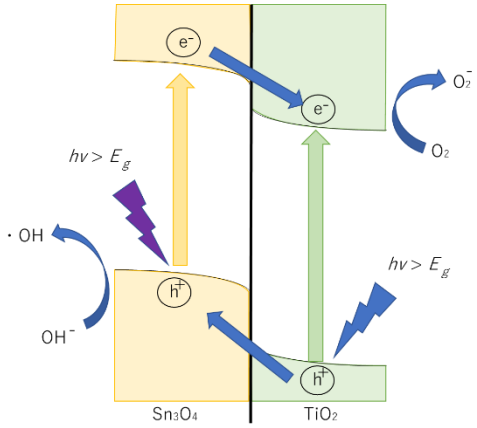

Fig. 4. A schematic diagram of the Sn_3O_4/TiO_2 heterostructure.

Fig. 4 shows a schematic diagram of the Sn3O4/TiO2 heterostructure. Band bending occurs at the junction interface between Sn_3O_4 and TiO_2 due to the difference in chemical potentials [24]; electrons excited by light in Sn_3O_4 move to TiO_2, and holes generated in TiO_2 move to Sn_3O_4. In the conduction band of TiO_2, electrons contribute to the reduction of O_2 to produce superoxide radicals, and in the valence band of Sn_3O_4, electrons react with H_2O to produce hydroxyl radicals. Therefore, the heterostructure is capable of providing excellent photocatalytic activity, which may have resulted in the higher bactericidal activity of $Sn_3O_4/TiO_2/SiO_2$ particles than TiO_2/SiO_2 particles.

However, the bactericidal performance of the particles with longer hydrothermal synthesis time was inferior to that of the particles with shorter hydrothermal synthesis time and TiO_2/SiO_2 only. This is due to

the fact that as the hydrothermal synthesis time increases, first, the thickness of the Sn_3O_4 film becomes thicker, and then its morphology becomes micro-flower. As a result, Sn_3O_4 was sufficiently irradiated with light to excite electrons, but the light energy received by TiO_2 was attenuated, resulting in the insufficient activity of the TiO_2 photocatalyst and difficulty in H_2O attachment to the TiO_2 surface, which resulted in the inability to take advantage of the heterostructure. In addition, the light energy reaching the TiO_2/SiO_2 core-shell structure inside the particles was attenuated, and the effectiveness of the light-scattering property could not be utilized, resulting in inferior disinfection performance compared to those with a short hydrothermal synthesis time. These results indicate that the attachment of an appropriate amount of Sn_3O_4 to TiO_2/SiO_2 particles with improved light-scattering properties affects the improvement of photocatalytic performance in indoor fluorescent light-irradiated environments and shows excellent potential as an efficient photocatalyst candidate.

4. Conclusion

We have prepared Sn_3O_4 heterojunction photocatalysts on TiO_2/SiO_2 particles with improved light utilization efficiency by hydrothermal synthesis. By adjusting the hydrothermal synthesis time, $Sn_3O_4/TiO_2/SiO_2$ particles with a controlled amount and shape of Sn_3O_4 can be prepared. The Sn_3O_4/TiO_2 heterostructure prepared by the hydrothermal reaction for 5 hours showed the highest photocatalytic disinfection performance under visible fluorescent light irradiation. The $Sn_3O_4/TiO_2/SiO_2$ heterostructure showed the highest photocatalytic sterilization performance under visible light irradiation.

Conflict of Interest

The authors declare no conflict of interest.

Author Contributions

Akihiro Yamazumi conducted the experiments and wrote the draft manuscript; Dang-Trang Nguyen helped with the research idea and experimental methods and edited the final paper; Kozo Taguchi advised on the research idea and experimental methods and finalized the manuscript; all authors had approved the final version.

References

[1] Kudo, A., & Miseki, Y. (2009). Heterogeneous photocatalyst materials for water splitting. *Chemical Society Reviews*, *38(1)*, 253-278.

[2] Dhananjay, S. B., Vishwas, G. P., & Anthony, A., B. (2002). Photocatalytic degradation for environmental applications - a review. *Journal of Chemical Technology and Biotechnology*, *77(1)*, 102-116.

[3] Guohui, C., Shaozheng, J., Yuanhua, S., Sujie, C., Yana, W., Pin, H., *et al*. (2015). Synthesis of scaly Sn_3O_4/TiO_2 nanobelt heterostructures for enhanced UV-visible light photocatalytic activity. *Nanoscale*, *7*, 3117-3125.

[4] Akira, F., & Kenichi, H. (1927). Electrochemical photolysis of water at a semiconductor electrode. *Nature*, 238, 37-38.

[5] Di, C., & Jinhua, Y. (2008). Hierarchical WO_3 Hollow Shells: Dendrite, Sphere, Dumbbell, and Their Photocatalytic Properties. *Advanced Functional Materials*, *18(13)*, 1922 -1928.

[6] Xuefei, W., Shufen, L., Huogen, Y., Jiaguo, Y., & Shengwei, L. (2011). Ag_2O as a new visible-light photocatalyst: Self-stability and high photocatalytic activity. *Chemistry A European Journal*, *17(28)*, 7777 -7780.

[7] Frank, M., Yu-C., T., Andrew, J., S., Barry, A., C, Daniel, T., Katherine, H., *et al*. (2001). Microwave activation

of electrochemical processes: enhanced PbO_2 electrodeposition, stripping and electrocatalysis. *Journal of Solid State Electrochem*, *5(5)*, 313-318.

[8] Debebrata, C. & Shimanti, D. (2005). Visible light induced photocatalytic degradation of organic pollutants. *Journal of Photochemistry and Photobiolgy C: Photochemistry Reviews*, *6(2-3)*, 186-205.

[9] Yan, L., Yong, C., Z. & Xiao, F., X. (2008). Hydrothermal synthesis and photocatalytic activity of CdO(2) nanocrystals. *Journal of Hazardous Materials*, *163(2-3)*, 1310-1314.

[10] Yunhui, H., Danzhen, L., Jing, C., Yu, S., Jiangjun, X., Xiuzhen, Z., & Peng, W. (2013). Sn_3O_4: A novel heterovalent-tin photocatalyst with hierarchical 3D nanostructures under visible light. *RSC Advances*, *4(3)*, 1266-1269.

[11] Jianling, H., Jianhai, T., Xingyang, L., Ziya, W., Yan, L., Quanshui, L., *et al.* (2017). Enhanced UV-Visible Light Photocatalytic Activity by Constructing Appropriate Heterostructures between Mesopore TiO_2 Nanospheres and Sn3O4 Nanoparticles. *Nanomaterials*, *7(10)*, 336.

[12] Xuefang, C., Ying, H., Kaichuang, Z., Xuansheng, F., & Chao, W. (2017). Novel hierarchical flowers-like Sn_3O_4 firstly used as anode materials for lithium ion batteries. *Journal of Alloys and Compounds*, *690(C)*, 765-770.

[13] Wei, X., Min, L., Xiaobo, C., Junhua, Z., Ruiqin, T., Rong, L., *et al*. (2014). Synthesis of hierarchical Sn_3O_4 microflowers self-assembled by nanosheets. *Materials Letters*, *120*, 140-142.

[14] Weiwei, X., Haoyu, Q., Xianghua, Z., Jing, D., Juan, W., & Qin, X. (2017). Visible-Light self-powered photodetector and recoverable photocatalyst fabricated from vertically aligned Sn_3O_4 nanoflakes on carbon paper. *The Journal of Physical Chemistry C*, *121(35)*, 19036-19043.

[15] Xiwang, Z., Tong, Z., Jiawei, N., & Darren, D., S. (2009). High-performance multifunctional TiO_2 nanowire ultrafiltration membrane with a hierarchical layer structure for water treatment. *Advanced Functional Materials*, *19(23)*, 3731-3736

[16] Tianyou, P., Akira, H., Jianrong, Q., & Kazuyuki, H. (2003). Fabrication of Titania tubules with high surface area and well-developed mesostructural walls by surfactant-mediated templating method. *Chemistry of Materials*, *15(10)*, 2011-2016.

[17] Jiajie, F., Li, Z., Jiaguo, Y., & Gang, L. (2012). The effect of calcination temperature on the microstructure and photocatalytic activity of TiO_2-based composite nanotubes prepared by an in situ template dissolution method. *Nanoscale*, *4(20)*, 6597-6603.

[18] Minmin, G., Liangliang, Z., Wei, L., O., Jing, W., & Ghim, W., H. (2015). Structural design of TiO_2-based photocatalyst for H_2 production and degradation applications. *Catalysis Science & Technology*, *5(10)*, 4703-4726.

[19] Yingjuan, X., Zhijiao, W., Qian, W., Min, L., & Lingyu, P. (2014). Effect of different base structures on the performance of the hierarchical TiO_2 photocatalysts. *Catalysis Today*, *225*, 74-79.

[20] Tim, L., Stuart, L., George, B., & Frank, G. (2012). Mesoporous hollow sphere titanium dioxide photocatalysts through hydrothermal silica etching. *ACS Applied Materials & Interfaces*, *4(11)*, 6062–6070.

[21] Jae-Won, L., Sungmin, K., Woo-Sik, K., & Jinsoo, K. (2007). Preparation and characterization of SiO_2/TiO_2 core-shell particles with controlled shell thickness. *Materials Chemistry and Physics*, *106(1)*, 39-44.

[22] Suim, S., Sun, H., H., Chanhoi, K., Ju, Y., Y., & Jyongsik, J. (2013). Designed synthesis of SiO_2/TiO_2 core/shell structure as light scattering material for highly efficient dye-sensitized solar cells. *ACS Applied Materials & Interfaces*, *5(11)*, 4815–4820.

[23] Yajun, W., Qisheng, W., Xueying, Z., Fengmei, W., Muhammad, S., & Jun, H. (2013). Visible light driven type II heterostructures and their enhanced photocatalysis properties: a review. *Nanoscale*, *5(18)*, 8326-8339.

[24] Hunter, M., Philip, E., H., Cheng-Lin, T., Kyekyoon, K., K., & Moonsub, S. (2011). Integration of type II nanorod heterostructures into photovoltaics. *ACS Nano*, 5(9), 7677-7683.

Akihiro Yamazumi was born in Japan in 1996. He received a B.E. degree in 2020 from the Department of Electrical and Electronic Engineering, Ritsumeikan University, Shiga, Japan. He is currently working towards a M.E. degree in science and engineering, Ritsumeikan University, Shiga, Japan. His current research interests photocatalysis and microbial fuel cells.

Dang-Trang Nguyen was born in Vietnam in 1986. He received a B.E. degree in 2009 from the Department of Telecommunication Systems Hanoi University of Science and Technology, Hanoi, Vietnam. After that, he received an M.E. in 2011 from the Department of Electronics and Electrical Engineering, Dongguk University, Seoul, South Korea. From 2011 to 2014, he completed his Dr. Eng. program in integrated science and engineering at Ritsumeikan University, Kyoto, Japan. After earning his Ph.D., he was a quality assurance engineer at Takako Industries, Inc. from Jul. 2015 to May 2017. He was a senior researcher at the Ritsumeikan Global Innovation Research Organization, Ritsumeikan University, from Jun. 2017 to Apr. 2020. Currently, he is an assistant professor at the Department of Electrical and Electronic Engineering, Ritsumeikan University. His fields of interest include Renewable Energy: Biofuel Cells, Solar Cells, Metal-based Batteries, and Hydrogen Energy.

Kozo Taguchi was born in Kyoto, Japan, on December 18, 1968. He received the B.E., M.E., and Dr. Eng. Degrees in electrical engineering from Ritsumeikan University, Kyoto, Japan, in 1991, 1993, and 1996, respectively. In 1996, he joined Fukuyama University, Hiroshima, Japan, where he had been engaged in research and development on the optical fiber trapping system, semiconductor ring lasers and their application for optoelectronics devices, and polymeric optical waveguides for optical interconnection. In 1996–2003, he worked as an assistant and lecturer in Fukuyama University. In 2003, he moved to Ritsumeikan University, Shiga, Japan, and currently he is a professor of department of electric and electronic engineering. From 2006 to 2007, he was a visiting professor at University of St Andrews (Scotland, United Kingdom). From 2014 to 2015, he was a visiting professor at Nanyang Technological University (Singapore). In 2019, he was a visiting professor at University of Bath (United Kingdom). His current research interests include cells trap, microfluidic cell-based devices, dye sensitized solar cell, biofuel cells, biosensors, and hydrogen energy. Dr. Taguchi is a member of the Japan Society of Applied Physics(JSAP) and the Electrochemical Society of Japan(ECSJ).